SolarPACES 2022, 28th International Conference on Concentrating Solar Power and Chemical Energy Systems
Analysis and Simulation of CSP and Hybridized Systems
https://doi.org/10.52825/solarpaces.v1i.639

Published: 15 Dec. 2023

Development of a PHIL Real-Time Simulation Testbed for Optimization of Hybrid Power Plant Generation

Jacob Wenner[1][https://orcid.org/0000-0002-4499-0144], Ben Bates[2][https://orcid.org/0000-0002-2728-7561], and Michael J. Wagner[3][https://orcid.org/0000-0003-2128-4658]

[1] Graduate Student, Department of Mechanical Engineering, University of Wisconsin-Madison

[2] Undergraduate Student, Department of Mechanical Engineering, University of Wisconsin-Madison

[3] Ph.D., Assistant Professor, Department of Mechanical Engineering, University of Wisconsin-Madison

Abstract. Future electrical grids will likely include a diverse group of power generation plants. With the growing list of new generation options comes many opportunities for more optimal energy production management and effective resource utilization. Microgrids are an ideal environment for research, development, and validation of those energy optimization strategies. This paper establishes a method for integrating a virtual thermal power plant model with a physical microgrid in a power hardware in the loop testbed. One advantage of these testbeds is their variety of configuration options. In this paper, the combined effects of photovoltaic and concentrating solar power generation are investigated. A conventional thermal power plant with components sized for CSP applications is modeled in the *Simscape* environment. Actual solar panels provide the photovoltaic element of this experiment. How the plant model and physical hardware interact is described in detail. A PV startup and shutdown event is simulated in real-time. The model responses are shown to be successfully and correctly coupled to electrical power flow in the testbed.

Keywords: Real-Time Simulation, Concentrating Solar Power, Hybrid Power Production, Dynamic Modeling

1. Introduction

As countries increase their dependence on renewable energy, power plants capable of steady, uninterrupted generation become crucial for maintaining a healthy grid. Hybrid generator systems offer an approach for providing dispatchable power by combining capabilities from multiple renewable technologies. Effective management of these proposed hybrid plants is complex, however, requiring advanced control strategies that must consider factors including efficiency, optimal dispatch, component stress, and frequency stability. Microgrid labs can be used to develop and validate those management strategies through power hardware in the loop (PHIL) testbeds. This paper describes a novel PHIL capability developed within an existing microgrid. PHIL capability enables physical hardware to interact with virtual environments (*or vice versa*) in real-time. The Wisconsin Energy Institute microgrid possesses a network of conventional inverters, resistive loads, solar panels, and PV inverters. However, the most prevalent form of power generation, large thermal plants, cannot physically exist in the lab for practical reasons. To address this limitation, large thermal plants can be emulated by means of a virtual plant model controlling a programmable power source. Via emulation, thermal plants can still interact in real-time with existing physical microgrid power equipment. The microgrid

testbed can investigate a diverse scope of dynamic energy generation scenarios. To demonstrate that idea, the scenario of hybrid photovoltaic (PV) and concentrating solar power (CSP) generation participating in a small grid has been developed and run in this PHIL testbed.

In regions with sufficient insolation, PV-CSP systems have been shown as a viable option for meeting a significant fraction of electrical demand [1]. Installing PV serves to cheaply increase the overall capacity of the system, as PV's levelized cost of electricity has become one of the lowest cost renewable energy solutions available [2]. CSP equipped with thermal energy storage adds long-duration storage and grid inertia to the system. Using an intermediate storage system such as molten salt, CSP plants have the potential to increase overall operating capacity factor and dispatchability. A CSP plant's synchronous generator adds physical inertia, thereby increasing system stability.

To describe how the microgrid PHIL testbed has been configured for the analysis and optimization of hybrid CSP-PV plant operation, the testbed can be grouped into two main sections; physical and virtual. The physical section includes the power sources, resistive load, and data acquisition devices that can be seen during the experiment. The virtual section consists of the steam generation system (SGS), turbine, governor control valve, governor controller, and generator inertia. A Rankine-cycle SGS is established as a basis for the thermal system. Finally, a PV-CSP load sharing test was performed. Experimental results show power measurements and corresponding CSP model reactions during a PV startup and subsequent shutdown event.

2. Real-Time Simulation

The various virtual and physical components presented in this paper have been integrated into one interactive testbed. Figure 1 shows the process flow of electrical power, model information, and operator setpoints. In the following sections, first the physical testbed components are described, next the physical component interactions are explained, and finally the virtual environment's CSP plant model and generator inertia model are discussed.

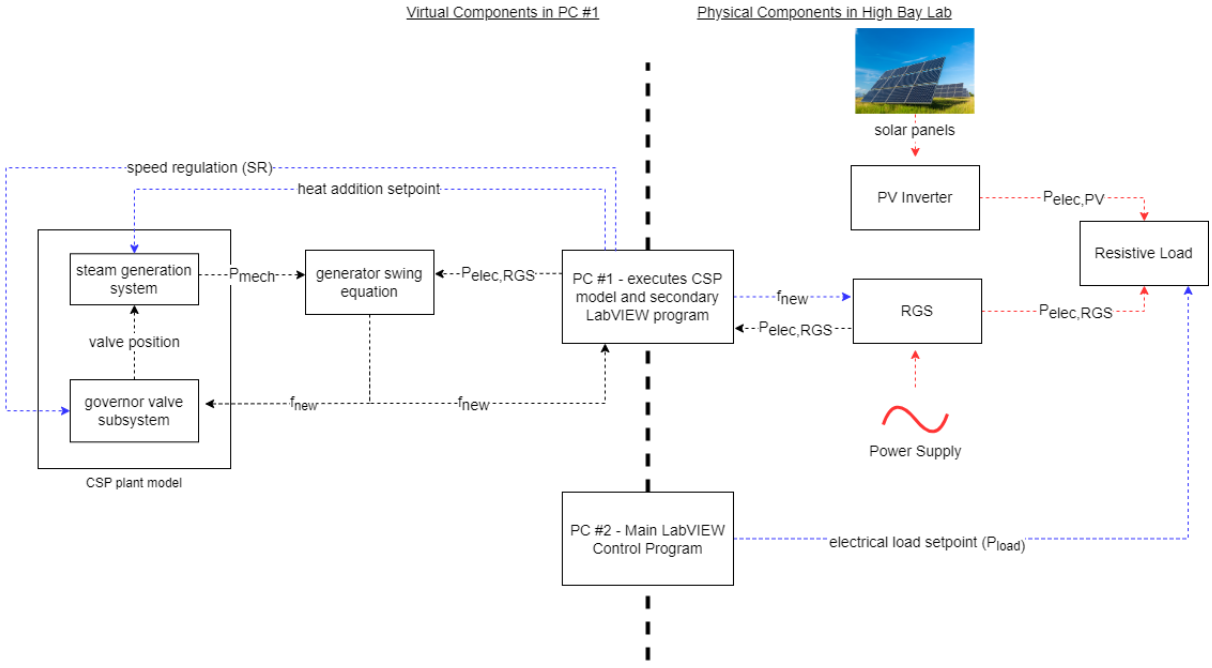

Figure 1. Real-time testbed configuration layout. The median dashed line indicates interface between the virtual and physical portions of this simulation.

2.1 Power Electronics Description

The Chroma Regenerative Grid Simulator (RGS) is a 45 kVA, fully programmable power source capable of outputting up to 480 V_{ac} line to line. Power flow is characterized as 'four-quadrant', which allows the generated voltage signal to either lead or lag the grid or reference voltage. Effectively, this allows the grid simulator to act as both a current sink or source. Since it is regenerative, any excess power in the testbed can be absorbed and safely fed back to the RGS' utility power source. The RGS can absorb or produce reactive power, the power needed to provide voltage support to the grid. Reactive power is an important aspect to include in grid stability studies because producing or absorbing reactive power is an important factor in providing grid services. Output voltage and frequency can be remotely set in real time via LabVIEW interface. Power flow can also be measured in real-time.

The PV inverter (PVI) used in this testbed was developed at UW-Madison, and it features a programmable interface. AC output voltage, reactive power droop, real power droop and AC output power setpoints can be changed between each experiment. It is programmed with phase locked loop (PLL) synchronization and maximum power point (MPP) tracking capability. Current and voltage measurements can be taken both on the DC supply side and the AC output side. The PVI can provide a maximum of 45 kW at voltages ranging between 208-480 V_{rms} line to line.

Typically, the PVI is supplied power from a *SunPower* PV array located on the rooftop of the Wisconsin Energy Institute. The solar panel array is capable of 6 kW maximum power output. Additionally, a Magna Photovoltaic Power Profile Emulator (PPPE) is capable of emulating solar panel sources up to 30 kW. When sufficient solar panel specifications and weather conditions are provided, the PPPE can emulate IV curves for providing realistic solar supply to the PVI.

Power produced by the PVI and RGS is dissipated in an Avtron resistive load, which is capable of rejecting up to 150 kW. Electrical load can be varied in discrete steps of resistance whose magnitude depend on the operating voltage. With an operating voltage of 120 V_{ac}, the load can be varied in steps of 0.9 kW.

2.2 Physical Testbed Configuration

Fig. 1 shows how these various components interact. The Avtron resistive load determines P_{load}, the electrical load that must be met by the combined outputs of the PVI and RGS at all times. The human operator at PC #2 sends load setpoints to the load during simulation. Power can flow between the PVI, RGS, and load via a common AC current conducting bus. The PVI provides a fraction of the total electrical load, and it can be powered by either the physical solar panels on the lab facility's roof or the Magna PPPE emulator. The PVI will maintain V_{ac}, the operating microgrid AC voltage, and hold its power output $P_{elec,PV}$ constant by adjusting its power angle. The RGS is the physical power source responsible for imitating the thermal power plant response. It is powered by a circuit connected to the utility grid. In contrast to the PVI, The RGS does not control its output power, $P_{elec,Chroma}$, but instead behaves as a constant voltage source with varying current output. This is similar to a synchronous generator, where the output AC voltage is held constant via automatic voltage regulation. As a result, if transmission losses are neglected, the RGS real power output will always be: $P_{elec,RGS} = P_{load} - P_{elec,PV}$. The RGS output voltage is always set to V_{ac} so that the PVI and RGS operating voltages match. The RGS also establishes microgrid electrical frequency by setting its own output frequency. Internal sensors calculate RGS real-time power output, $P_{elec,RGS}$. This measurement is passed every 1 s to PC #1, where it is then passed on to the virtual testbed portion as an input to Eq. 1. The calculated electrical frequency, f_{new} and $P_{elec,RGS}$ are related via Eq. 1 and this is explained in the modeling methodology section. Ultimately, electrical frequency is updated to f_{new} every 1 s. This timestep gave the PVI sufficient time to resynchronize to frequency changes, and it reduced model instabilities in PC #1. PC #2 is responsible for controlling main

electrical contactors for all power electronic equipment, collecting voltage and current waveforms, and commanding the electrical load setpoint. This is accomplished via a main *LabVIEW* control and data acquisition program.

2.3 Virtual Testbed Configuration

PC #1 can be thought of as a gateway between the physical and virtual testbeds. PC #1 contains all sections of the virtual model in a compiled Simscape model [3]. Simscape is a Matlab Simulink toolbox that enables a user to create thermal models using library component blocks. Simscape constructs a system of equations for the model based on all physical and signal connections. The resulting equations are mapped into a state vector describing the entire model. After initialization, the Simscape solver performs a transient solve of the model by integrating all differential equations. The model was solved at constant time steps of 100 ms. Although a brief overview of the Simscape simulation process has been provided in this paper, the complete explanation can be found in [4].

Both the CSP plant model and generator inertia are considered in the *Simscape* model. The CSP plant model can be further separated into the SGS and governor valve subsystems. During experiments, PC #1 runs a *LabVIEW* program that concurrently executes the *Simscape* model, outputs f_{new} setpoints to the RGS, and passes $P_{elec,RGS}$ input measurements back to the *Simscape* model. The synchronous generator compares the CSP plant model's calculated turbine power, P_{mech} and measured RGS power output $P_{elec,RGS}$. The generator submodel calculates the resultant frequency, f_{new}. This value is an output to the RGS, which updates its frequency; f_{new} is also an input for the CSP plant model. The governor valve subsystem changes valve position based on frequency changes. Controls and equations for the CSP plant model are described in the modeling methodology section. The human operator controls heat input and speed regulation setpoints for the CSP plant in real-time, similar to control of an actual power plant. In the next section the power block components of the CSP plant model are described.

3. Modeling Methodology

The virtual portion of this testbed is comprised of a SGS, turbine, governor control valve, governor control, and generator inertia model. A dynamic model of the power block was developed in *Matlab Simulink* workspace with the *Simscape* toolbox [3]. Each subsystem seen in Fig. 2 has different dynamic effects to consider. Steam drum volume, superheater's steam tube volume, and controller dynamics are all considered in the SGS model. The turbine subsystem considers inertial effects and off-design operation. The control valve subsystem considers system lag due to inherent valve travel time.

3.1 Steam Generation System

The following discussion of the SGS does not provide a full description of the conventional aspects of the model, but instead focuses on factors affecting the CSP plant's dynamic performance. Initial values for states 1-6 correspond to steady state operating points of a conventionally designed Rankine-cycle CSP plant capable of providing approximately 45 MW of gross turbine power.

The SGS model includes a feedwater pump, boiler, and superheater. A diagram of the modeled SGS can be seen in Figure 2. Feedwater heating and condenser dynamics have not been considered. These dynamics would affect the state of feedwater entering the boiler. Additionally, the thermal heat capacitance of all SGS components were also neglected. Including heat capacitance effects would likely cause steam state changes to lag further behind the corresponding plant operational changes. Although these details certainly warrant further modelling and research, the dynamic Rankine-cycle plant shown in Figure 2 was primarily built to

provide initial experience with the PHIL integration process. Once a method for integrating CSP models with PHIL equipment has been established, more resources can be dedicated to adding model complexity.

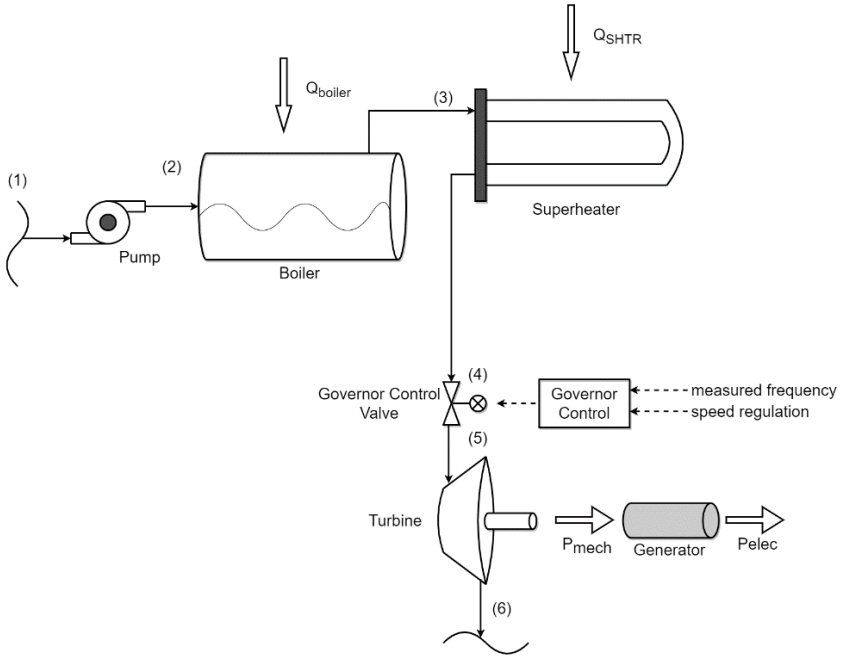

Figure 2. Flow and control schematic for CSP plant model.

Feedwater was assumed to enter the system at a fixed enthalpy of 1450 KJ/kg and pressure of 110 bar. An isentropic pump regulates mass flow rate and pressurizes the feedwater up to boiler pressure, which is approximately 120 bar. The boiler represents a evaporator heat exchanger and steam drum with a total combined volume of 50 m^3. The boiler volume has a large impact on variability of drum level, the amount of liquid in the steam drum. Drum level is of particular interest, since excessively low drum levels result in equipment damage and high levels result in low steam volume. Liquid level is monitored and passed as feedback to the human operator during simulation. Since the pump pressure determines liquid flowrate into the drum at state 2, the pump is a suitable control to maintain an acceptable drum level. The model constrains all mass flow leaving the boiler at state 3 to be steam with quality x=1, which represents the steam separators present in actual steam drums. The superheater has a steam-side volume of 1.7 m^3. As shown in Fig. 1, the heat input setpoint is an input provided to the CSP plant model by the human operator during real-time simulation. Heat input includes $\dot{Q}_{boiler}$ and $\dot{Q}_{SHTR}$ (shown in Fig. 2), the respective heat flows supplied to the boiler and superheater during operation.

3.2 Turbine Governor Valve

The governor control valve between states 4 and 5 determines the inlet pressure and steam mass flow into the turbine. The characteristics of this valve and its control are of primary importance in determining the plant's dynamic behavior, and as such are sometimes used alone to estimate response [5]. The governor valve model and control, shown in Fig. 3, is primarily composed of frequency response elements and a servo-motor subsystem. This model is based on existing models found in [5].

The governor control incorporates primary and secondary response elements by changing the governor control valve position in response to either deviations of the electrical frequency (f_{new}) or to new target frequency speed regulation (SR) setpoint signals. The “measured frequency” input in Fig. 3, corresponds to f_{new} in Fig. 1. The error between measured and

reference frequency causes a primary droop response. The SR input is typically a slower secondary response that can be manually set by human operator to correct for any steady state electrical frequency error and represents automatic generation control (AGC) input to the system, which is typically a signal sent by a grid operator in response to significant load changes. The model combines both primary and secondary signals into a commanded valve position change which is then multiplied by a droop response gain block, K_g. This control scheme ultimately changes valve position to elicit a mass flow and pressure response which consequently increases or decreases gross turbine output power. This power change will address any imbalance between turbine power output (P_{mech}) and generated electrical power output (P_{elec}).

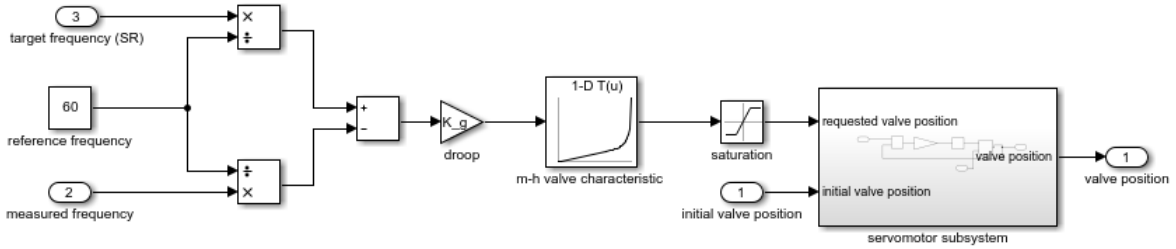

Figure 3. Valve controller with frequency input, characteristic curve prediction, and the valve's servo-motor subsystem.

The mass flow (m) versus openness (h) valve characteristic block helps predict valve behavior and improves controller stability. Even if the valve is oversized, the m-h block accounts for this by adjusting the commanded valve position change to be smaller when the valve is mostly closed. The saturation block enforces reasonable values for the governor controller by limiting requested valve position between 1 (fully open) and 0 (fully closed). Although the electrical control signal could transmit almost instantly to the valve actuator, there will be a lag between requested position and actual position due to actuator travel time, which can be significant depending on the valve in use. To estimate this lag, a servomotor subsystem was built as shown in Fig. 4. The requested valve position is pushed into a feedback loop as shown using a gain constant TSM=0.1 [5]. The saturation block enforces valve servo rate limits - i.e., the maximum speed at which the valve can change position. This valve has a maximum speed of 0.2 p.u./s which limits position change to no more than 20% every second.

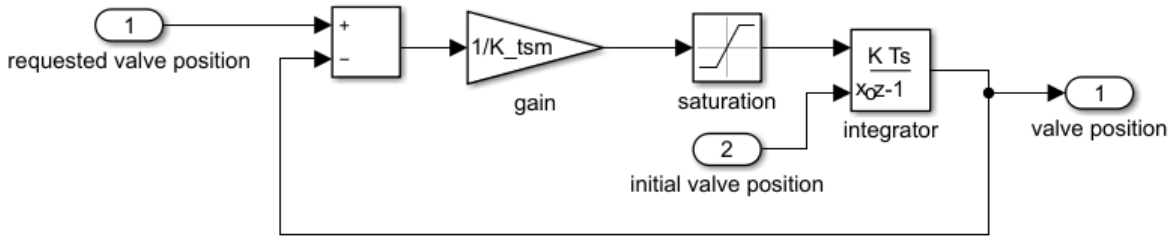

Figure 4. Governor valve servomotor model to capture valve actuation time delay.

Input from Fig. 4 is passed to the actual valve. The valve is modeled using a variable local restriction block in Simscape. The discharge coefficient is C_v=0.25. The valve position command, shown as an output in Fig. 4, is scaled from a per unit value to an actual restriction surface area using a pipe area gain constant. The actual valve block and valve area gain constant are not shown in Fig. 4. The valve itself is represented in Simscape by a variable local restriction block. Thorough documentation of the valve equations can be found in [6].

3.3 Turbine and Generator Inertia

In a power plant, the turbines and synchronous generators are mechanically coupled together; mechanical torque from the steam turbine drives the generator, which is producing an opposing electrical torque. When the combined mass' rotational frequency does not vary largely from 60 Hz, torque is proportional to power. Rotational frequency remains constant when P_{mech}=$P_{elec.}$ However, if these two powers are unequal, the combined rotating mass will either accelerate or decelerate. This leads to the well known swing equation, which defines an electrical system's change in electrical frequency in terms of the mechanical power input, electrical power drawn, and the physical inertia present in the system [7]. If load damping frequency responses and parasitic power losses are neglected, the result is shown in Eq. 1 where P_{elec} is the total electric load, P_{mech} is the mechanical power produced by the turbine, H is the inertia constant, f_0 is the nominal frequency of 60 Hz, and S_B is the total rated generation power of the system.

$$\frac{df}{dt} = \frac{f_0}{2HS_B}(P_{mech} - P_{elec}) \quad (1)$$

A grid inertia constant value of H=6 s is used in this model. P_{elec} in Eq. 1 is the real-time measured electrical power output $P_{elec,RGS}$ shown in Fig. 1. Thus, P_{elec} comes from the physical testbed. The turbine's power output is calculated in *Simscape*. It is scaled from specified nominal operating conditions based on Stodola's ellipse relation [8].

Eq. 1 is used to represent the total grid inertia in *Simscape*. S_B for the entire grid in consideration was 900 MW. The rated electrical capacity of the modeled CSP plant was 40 MW. Therefore, the CSP plant was responsible for meeting approximately 4.5% of the grid's electrical load. All other generation plants were assumed to be ideal, load following sources. Thus, the calculated frequency change from Eq. 1 would solely depend on the CSP's load following effectiveness. During lab simulation, Eq. 1 can be integrated to solve for the change in frequency over a given time step. By assuming an initial electrical system frequency of 60 Hz, the model can always integrate known conditions for the resulting electrical frequency (f_{new}).

4. Results

A simple loading scenario was run to evaluate testbed performance. This experiment investigates the response of CSP plants during periods of high PV grid penetration. The results presented in this paper were generated using the following procedure. The resistive load setpoint is held at 5 kW for the entirety of the experiment. From 0-320 s, this resistive load is completely met by the RGS. Then, at approximately 320 s, the PVI is turned on with an output setpoint of approximately 0.75 kW. Since the RGS is acting as a constant voltage source, its output naturally decreases while the PVI is producing power. Around 475 s the PVI is turned off. The RGS output then supplies 100% of the resistive load. The electrical power data is shown in Fig. 5. It should be noted that limits on RGS data acquisition accuracy result in some variance in measured RGS real power output. However, the variance was not significant enough to affect the overall experimental trends and its effects can be reduced by performing higher power tests in the future. The reader will also note that before the PVI begins producing power, its measured power output is negative. This is a resistive parasitic electrical loss at the PVI microgrid connection.

The measured RGS power output seen in Fig. 5 is scaled according to a 5 kW:40 MW ratio and passed as model input to the virtual side of the testbed every 1 s. As explained in the modeling methodology section, P_{elec} factors into CSP plant response and calculated grid frequency. On the virtual side, any model states can be output and recorded. Calculated plant power, valve area, mass flow, turbine inlet pressure, boiler pressure, and drum level are recorded during this experiment. These states of interest along with heat input and scaled RGS electrical power, are shown in Fig. 6.

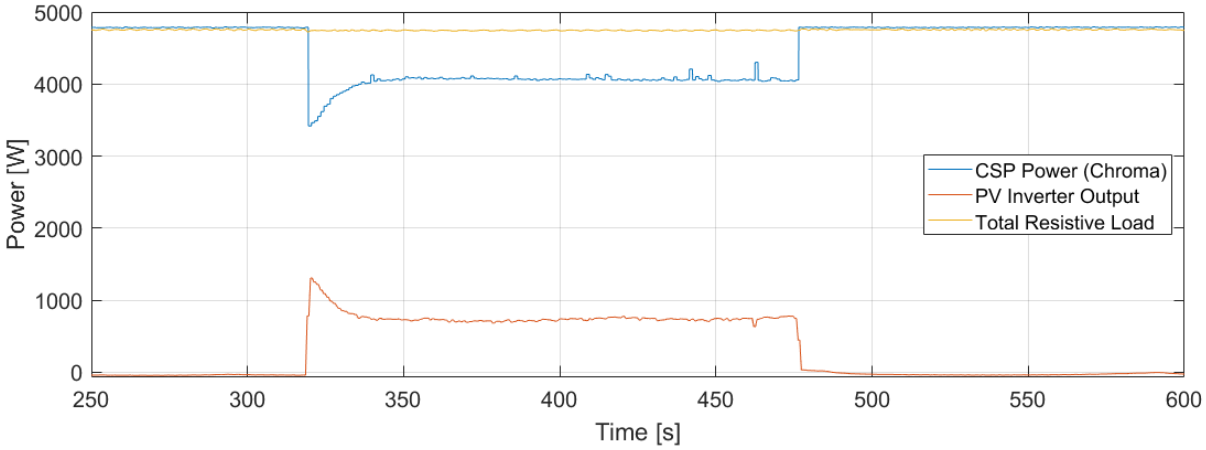

Figure 5. Active power measurements from real-time test. The RGS and PVI jointly supply power to the load from 320 s to 475 s.

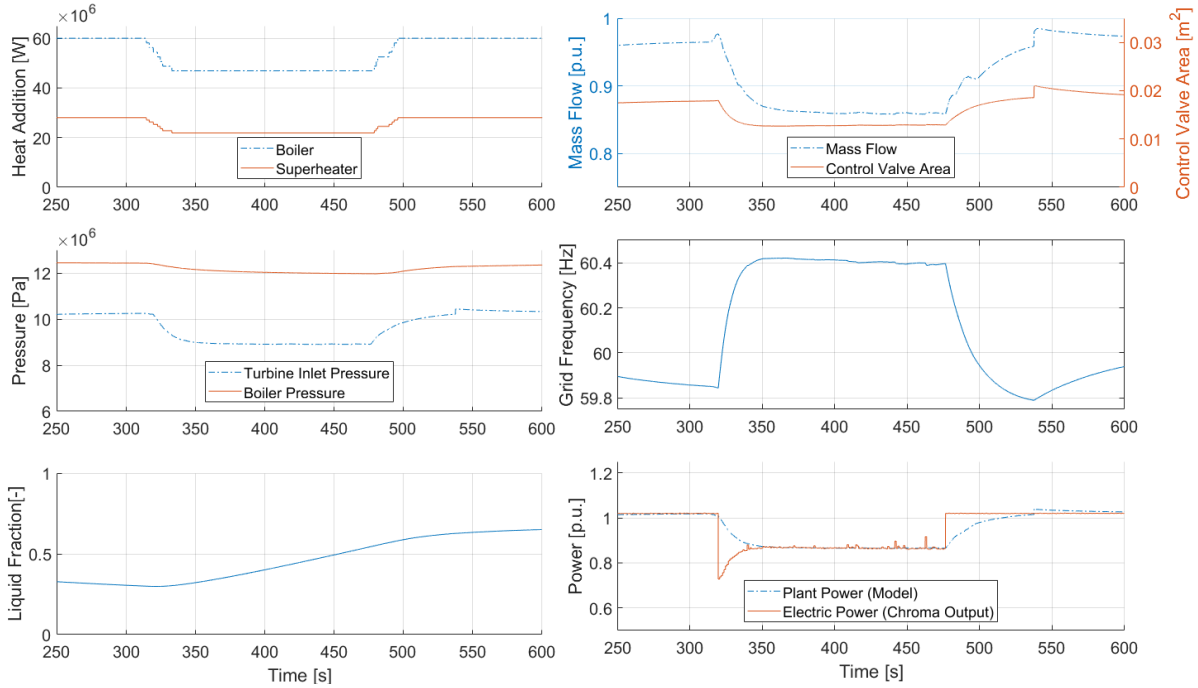

Figure 6. Real-time model results from PHIL test shown in Fig. 5.

Fig. 6 demonstrates that the thermal model responds to real-time electrical power balancing between the PVI and RGS. In general, model states behave as expected when exposed to real-time signal. It can be observed that the valve response is directly correlated to system mass flow. The grid frequency and power output plots show that when calculated CSP P_{mech} lags the electric power, the grid frequency changes according to Eq. 1. The heat input varies as it is manually adjusted via human operator in response to the load change. This impacted mass flow by increasing or decreasing steam production. It can also be observed that the governor valve causes the turbine to experience larger pressure fluctuations compared to the boiler.

The effect of the proportionally large PV system size can be clearly seen during PVI startup and shutdown. The primary CSP response at PVI startup and shutdown is largely influenced by speed control. The secondary response depends primarily on heat addition and speed regulation setpoints. Just before 550 s, speed regulation setpoint is increased, providing

a temporary boost in power output for grid frequency correction. The liquid drum level is sensitive to pump pressure and heat addition. When the CSP's operating point is reduced due to PV production, the operating point shift results in a steam drum flow imbalance. Since steam is being produced at a rate lower than the mass flow rate of feedwater, the drum level begins to increase. This issue can be addressed by fine-tuning the pump pressure, and consequently, feedwater flow.

5. Summary

Solar panels, an experimental inverter, resistive load, and a regenerative grid simulator have been operated in an electrically synchronized experiment with coordinated control. A simple rankine cycle model has also been defined, implemented in *Simscape*, and integrated into the control of a programmable power source. The virtual model was successfully run in a real-time communication setting with power hardware in the loop components and offered insight into thermal plant response when coupled with PV inverters. A method has been established for evaluation of PV-CSP interaction and performance in electrical grids, which enables future investigation of curtailment strategies, operational recommendations and training, component degradation, optimal energy storage management, and effects of cloud cover.

Data availability statement

Data is available on request from the author.

Author contributions

Jacob Wenner: methodology, conceptualization, investigation, validation, visualization, formal analysis, and writing – original draft. Michael J. Wagner: project administration, conceptualization, funding acquisition, resources, supervision, and writing – review & editing. Ben Bates: formal analysis, investigation and visualization.

Competing interests

The authors declare no competing interests.

References

1. E. Ghirardi, G. Brumana, G. Franchini, and A. Perdichizzi, “The optimal share of PV and CSP for highly renewable power systems in the GCC region,” Renewable Energy, vol. 179, pp. 1990–2003, 2021, doi: https://doi.org/10.1016/j.renene.2021.08.005
2. Feldman, David, Vignesh Ramasamy, Ran Fu, Ashwin Ramdas, Jal Desai, and Robert Margolis. 2021. “U.S. Solar Photovoltaic System Cost Benchmark: Q1 2020“. Golden, CO: National Renewable Energy Laboratory. NREL/TP-6A20-77324. https://www.nrel.gov/docs/fy21osti/77324.pdf
3. The MathWorks Inc. version 9.8.0 (R2020a), “MATLAB Simulink and Simscape Toolbox.” Natick, Massachusetts, 2020.
4. Mathworks, “How Simscape Simulation Works.” 2022. Available: https://www.mathworks.com/help/physmod/simscape/ug/how-simscape-simulation-works.html (Accessed: Sep. 13, 2022. [Online])
5. Pourbeik, P. “Dynamic Models for Turbine-Governors in Power System Studies” 2013.
6. Mathworks, “Variable Local Restriction (2P).” 2015. Available: https://www.mathworks.com/help/physmod/simscape/ref/variablelocalrestriction2p.html#:~:text=The%20Variable%20Local%20Restriction%20(2P,specified%20as%20a%20physical%20signal (Accessed: Sep. 13, 2022. [Online])

7. M. Eremia and M. Shahidehpour, Handbook of electrical power system dynamics: modeling, stability, and control, vol. 92. John Wiley & Sons, 2013.
8. Stodola, Steam and Gas Turbines, vol. translated. P. Smith, New York, 1945.